Shadow index estimation algorithm development and improvement

Masao MORIYAMA (Nagasaki Univ.)

19 Jan. 2022

Contents

1. Shadow index definition and estimation algorithm
2. Validation results
3. Application: Broadleaf/Needleleaf forest discrimination

Canopy and Shadow

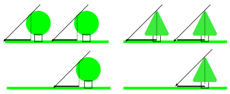

⇒ Shadow area reflects the leaf and canopy type.

Definition

Land leaving radiance from a pixel

$I_s=(F_r\cos(\theta_s')+F_d)\frac{\rho}{\pi}$, (if $\theta_s'>\pi/2, \cos(\theta_s')=0$)

F_r: direct solar irradiance, θ_s': average incident angle, F_d: diffuse solar irradiance, ρ: average surface reflect ance ⇐ Direct reflection contains the shadow

Reflectance scale up

$I_s=\sum[w_i(F_r\cos(\theta_{si}')+F_d)\frac{\rho_i}{\pi}]=(F_r\cos(\theta_s')+F_d)\frac{\rho}{\pi}$,

(w_i: area proportion of the ith subsurface)

Assumptions

1. Each subsurface within a pixel has the same reflectance ρ_i and incident angle θ_{si}'.
2. F_d is negligible. (SWIR, SGLI/SW03: 1.6[μm])
3. $\sum[w_iF_r\cos(\theta_{si}')\frac{\rho_i}{\pi}]=F_r\cos(\theta_s')\frac{\rho}{\pi}$, $\sum[w_iF_d\frac{\rho_i}{\pi}]=F_d\frac{\rho}{\pi}$

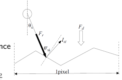

Definition of the average surface reflectance: $\rho=\sum w_i\rho_i$

Definition of the average incident angle: $\cos(\theta_s')\rho=\sum w_i\cos(\theta_{si}')\rho_i$

Definition (*contd.*)

Relationship between the shadow content and $\sum w_i\cos(\theta_{si}')\rho_i$

ρ_i	Uniform random number within the range of 0.05 – 0.1, 0.15 – 0.3, 0.25 – 0.5, 0.35 – 0.7, 0.45 – 0.9
w_i	Uniform random number within the range of 1.0×10^{-10} – 1.0×10^{-6}
$1-\cos(\theta_{si}')$	Log–normal distribution with the average of 0.1 – 0.9 and the standard deviation of 0.2, 0.4, 0.6
Cast shadow	Uniform random number within the range of 0 – 0.01, 0 – 0.05, 0 – 0.1

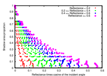

$$SDI=\exp(c\,\rho_{SW03}\cos(\Theta_s))$$

c: Coefficient (Average reflectance $\bar{\rho}$ included) ← Defined from the ground truth,

Θ_s: Incident angle (Solar zenith)

SGLI Shadow Index product (SDI)

- Assumption 1: Neglect the diffuse solar irradiance → 1.6[μm] (SW03) and not hazy aerosol condition.
- Assumption2: For the vegetation area. In the case of NDVI < 0.75, On the QA field, Non–vegetation flag is assigned.
- Coeff. definition and validation: From LPC (USGS/3DEP) and the solar geometry at the observation, the shaded area within a pixel is computed.

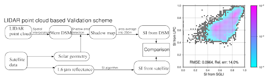

Examples

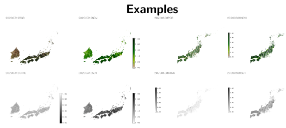

SDI and forest type: Shirakami beech forest

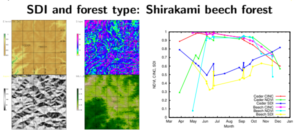

⇓

Solar incident angle $\cos(SZA)\cos(Slope)+\sin(SZA)\sin(Slope)\cos(Aspect-SAZ)$ dependency

Comparison between JAXA/HRLULC

JAXA/HRLULC(High Resolution Land Use Land Cover): 10[m] resolution land use land cover dataset

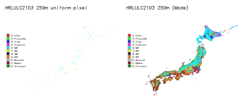

Class	Number	Class	Number
Urban(2)	916	DNF(7)	58635
Paddy(3)	195879	EBF(8)	18124
Crop(4)	89768	ENF(9)	3246163
Grass(5)	317577	Bare(10)	1638
DBF(6)	3283052	Banboo(11)	335

- Select the uniform category within SGLI 250[m] pixel
- 2019/07 to 2020/12, Daily SDI are averaged

Comparison between JAXA/HRLULC (*contd.*)

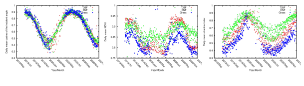

- Incident angle (≃ Solar zenith) dependency
- SDI becomes smaller: Needle leaf→Broad leaf→Grass
- SDI difference from the forest type: High solar elevation season

⇓

SDI based forest type variable with low incident angle dependency

SDI based forest type variable: LDSDI

⇒ Linear discriminant function for DBF and ENF seration usinf SDI and incident angle.

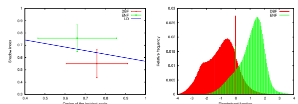

$$LD_{SDI}=3.357\cos(\Theta_s)+11.60SDI-9.965$$

Accurady 85% (ovberall years)

LDSDI

入射角余弦との相関が低い

Class	SDI	LD_{SDI}
DBF	-0.630056	-0.295103
ENF	-0.706243	-0.255804
All	-0.642731	-0.373973

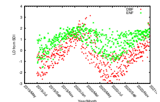

LDSDI

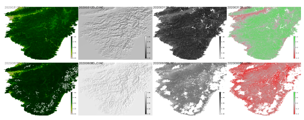

⇓

Less incident angle dependency but still remained → Limited use at the high solar elevation season

Summary and the future plan

1. SDI version 3 is developed and validated.
2. For the forest type discrimination, SDI and solar incident angle based variable is defined and shows the probability of the forest type discrimination in the high solar elevation season.
3. LPC based validation will be continued. (Not only 3DEP, but Japanese local government provided LPC)
4. LANDSAT SDI will be developed for the indirect validation.
5. LDSDI will be refined for the VRI → AGB coefficient definition.

LST estimation algorithm development and improvement

Masao MORIYAMA (Nagasaki Univ.)

19 Jan. 2022

Contents

1. GCOM–C/SGLI LST product error analysis
2. Effect of the time difference between the observation and the numerical forecasting data.
3. Summary and future

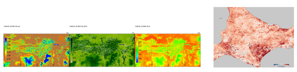

SGLI/LST estimation algorithm

Inputs: Brightness temp. T_1, T_2,
Radiation parameters from the numerical forecasting data τ, I_a, F
Unknowns: $\varepsilon_1, \varepsilon_2, T_s$

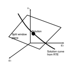

$$f_1=B_1^{-1}\{\tau_1(\theta)[\varepsilon_1B_1(T_s)+(1-\varepsilon_1)\frac{F_1}{\pi}]+I_{a1}(\theta)\}-T_1=0$$

$$f_2=B_2^{-1}\{\tau_2(\theta)[\varepsilon_2B_2(T_s)+(1-\varepsilon_2)\frac{F_2}{\pi}]+I_{a2}(\theta)\}-T_2=0$$

$$f_3=C_0+(C_1+r_1C_2)T_1+C_3r_1+(C_4+r_2C_5)T_2+C_6r_2-T_s=0,\quad (r_i=1-\varepsilon_i)$$

Third formula: Split window

⇓ Newtonian iteration

$J=\sqrt{f_1^2+f_2^2+f_3^2}\to min.$, $T_s,\varepsilon_1,\varepsilon_2\to$: solution

$J\le1$[K]: Converged, $1<J\le2$[K]: Semi–converged, $J>2$[K]: Non–converged → QA

RTC, Split window

Simplified radiative transfer code

Precipitable water, Surface air temperature: Inputs ξ: Optical thickness($\tau(\theta)=\exp(-\xi/\cos\theta)$), $I_a(\theta)$: Path radiance F: Downward irradiance at the surface.

Split window

3 coeff. sets.

Profile: ECMWF 2000 Monthly mean profile (averaged over 10 [deg.] latitude interval)
Surface temperature: Air temperature at the surface + 0, 5, 10, 15, 20, 25, 30, 35, 40[K]
$\bar{\varepsilon}$: 0.95, 0.96, 0.97, 0.98, 0.99, 1
a: -0.5, 0.25, 0, 0.25, 0.5
Observation zenith: 0, 15, 30, 45[deg.]
Observation error: 0 (for RTC and Split window), Nominal NEdT(0.1[K]@300[K], for LST estimation)

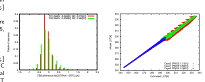

LST estimation from the simulated data

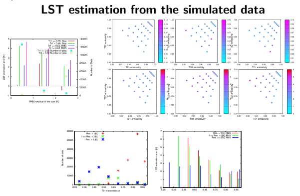

Validation result from the longwave radiation data at the flux site

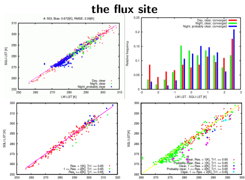

2019/09/01 RRV, 2020/08/11 KANTO

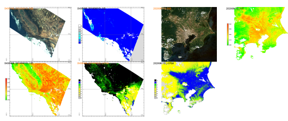

Numerical forecaseting data

From JMA GPV/GA (00, 06, 12, 18UTC, 0.5°) at the nearest time of the observation → The surface air temperature and the precipitable water → Transmittance, Path radiance and downward irradiance → 3D bilinear interpolation at each pixel

⇓

course resolution and maximum 3hours time difference

Atmospheric data error → LST estimation error

Sensitivity analysis of the atmospheric data error

Add the offset to the simulation data(Air temperature + 1, 2, 3[K], Precipitable water × 0.95, 0.90, 0.85) → Convergency and LST estimation error.

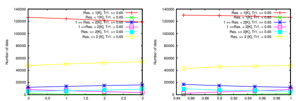

Copnvergency: Air temperature, Precopitable water → no significant change.

Sensitivity analysis of the atmospheric data error

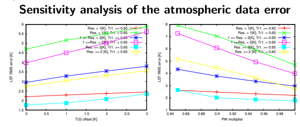

LST RMSE: Air temperature, Precopitable water → getting worse under the low transmittance condition

Comparison between AMeDAS and numerical forecasting surface air temperature

- Numerical forecasting data: NCEP Reanalysis2(d083.2) 1[deg.], 00, 06, 12, 18UT
- AMeDAS: The difference between the 1 [deg.] averaged elevation and the observatory elevation is within 10[m], at 11, 23 JST

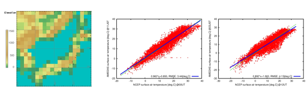

⇒ Seems certain dependency but more precise analysis is necessary.

Summary and the future plan

1. From the numerical simulation data, The large LST estimation error conditions are clarified.
2. The time difference between the observation and the numerical forecasting data affects the LST estimation error under the low transmittance condition.

3. To make ease the interpretation of the LST estimation error from the QA and the estimated emissivity,
4. To compensate or notify the time difference effect, the analysis of the surface air temperature effect under the complete clear condition.